徐鑫,刘阳,张勇,等.大兴安岭东坡中北段六九山斑岩铜成矿系统浅成岩成因与地球动力学背景.吉林大学学报(地球科学版),2024,54(5):1558-1574. doi:10.13278/j.cnki.jjuese.20230245.

Xu Xin, Liu Yang, Zhang Yong, et al. Genesis and Geodynamic Setting of Hypabyssal Intrusive Rocks in the Liujiushan Porphyry Cu Ore System, Eastern Edge of the Northern Great Hinggan Range. Journal of Jilin University (Earth Science Edition), 2024,54(5):1558-1574. doi:10.13278/j.cnki.jjuese.20230245.

大兴安岭东坡中北段六九山斑岩铜成矿系统浅成岩成因与地球动力学背景

徐 鑫[1],刘 阳[1],张 勇[2],褚小磊[1],徐智恺[1],孙景贵[1],刘 晨[3]

1.吉林大学地球科学学院,长春 130061
2.中国地质科学院矿产资源研究所,北京 100037
3.长春工程学院党委组织部,长春 130012

摘要:六九山铜矿床产在大兴安岭地区东坡中北段,位于中亚造山带东端。为了探讨该区浅成岩成因与地球动力学背景,对六九山斑岩铜成矿系统内与成矿密切的闪长玢岩、二长斑岩两类浅成岩进行了地质、岩相学、锆石U-Pb同位素定年和元素地球化学等方面的研究。结果表明:闪长玢岩和二长斑岩内岩浆锆石加权平均年龄分别为(132.6±2.6)Ma(n=5)和(132.4±1.3)Ma(n=22),岩浆就位发生在约132 Ma,结合辉钼矿Re-Os同位素年龄((134.1±0.8)Ma),限定成矿作用发生在早白垩世;闪长玢岩($w(SiO_2)$为52.98%~59.83%)和二长斑岩($w(SiO_2)$为66.90%~67.56%)为典型的中—酸性浅成斑岩,富集大离子亲石元素,亏损高场强元素,分别为典型岛弧钙碱性岩和埃达克质岩石;岩浆起源于与大洋板块俯冲有关的以流体交代为主的富集地幔部分熔融;成岩成矿作用适值中生代早白垩世库拉板块向欧亚板块俯冲的大陆边缘岩浆弧背景。

关键词:成岩时代;元素地球化学;斑岩铜成矿系统;岩石成因;地球动力学;六九山铜矿床;大兴安岭

doi:10.13278/j.cnki.jjuese.20230245 **中图分类号**:P595;P581 **文献标志码**:A

Genesis and Geodynamic Setting of Hypabyssal Intrusive Rocks in the Liujiushan Porphyry Cu Ore System, Eastern Edge of the Northern Great Hinggan Range

Xu Xin[1], Liu Yang[1], Zhang Yong[2], Chu Xiaolei[1], Xu Zhikai[1], Sun Jinggui[1], Liu Chen[3]

收稿日期:2023-10-05

作者简介:徐鑫(1989—),男,硕士研究生,主要从事矿床学方面的研究,E-mail:275046224@qq.com

通信作者:张勇(1982—),男,研究员,主要从事矿床地球化学方面的研究,E-mail:yongzhangcc@163.com

基金项目:国家自然科学基金项目(42072085,41172072,40772052,40472050,41390444);中国地质调查局项目([2023]02-23-06);国家重点研发计划项目(2017YFC0601306)

Supported by the National Natural Science Foundation of China (42072085, 41172072, 40772052, 40472050, 41390444), the Project of China Geological Survey ([2023]02-23-06) and the National Key Research and Development Program of China (2017YFC0601306)

1. *College of Earth Sciences*, *Jilin University*, *Changchun* 130061, *China*
2. *Institute of Mineral Resources*, *Chinese Academy of Geological Sciences*, *Beijing* 100037, *China*
3. *Party Committee Organization Department*, *Changchun Institute of Technology*, *Changchun* 130012, *China*

Abstract: The Liujiushan Cu deposit is located in the eastern end of the northern Great Hinggan Range, part of the easternmost edge of Central Asian orogenic belt. This study presents detailed field geology, petrography, elemental geochemistry and geochronology of diorite porphyry and monzonite porphyry to reveal the petrogenesis and geodynamic setting of these intrusive rocks. Magmatic zircons from diorite porphyry and monzonite porphyry yielded a weighted average age of (132.6±2.6) Ma (n=5) and (132.4±1.3) Ma (n=22), respectively. The LA-ICP-MS zircon U-Pb ages show these intrusive rocks were emplaced at ~132 Ma, consistenting with the molybdenite Re-Os isotopic dating of (134.1±0.8) Ma, which constrains Cu mineralization to the Early Cretaceous. The diorite porphyry (52.98%-59.83% $w(SiO_2)$) and monzonite porphyry (66.90%-67.56% $w(SiO_2)$) are classified as intermediate to acidic hypabyssal intrusive rocks, enriched in the large ion lithophilic elements and deleted in high field strength elements, representing island arc alkaline and of adakitic rock types, respectively. Their parental magmas originated from an enriched mantle. All these studies show that the diagenesis and mineralization resulted from subduction of the Kula slab beneath Eurasian continent.

Key words: diagenesis age; elemental geochemistry; porphyry Cu ore system; petrogenesis; geodynamic; Liujiushan Cu deposit; Great Hinggan Range

0　引言

铜广泛应用于建筑、电器、电子工业、机械制造、运输设备和日用消费等领域，铜矿是有色金属矿产资源的重要组成之一，是我国目前对外依存度较高的矿产[1]。六九山铜矿床是近年来在大兴安岭东坡中北段勘探出的中型铜矿床，其工业类型为爆破角砾岩型铜矿床[1]。矿床成因类型起初认为是斑岩型铜矿床[2]，后期认为是浅成热液高硫化型铜矿床[3-4]；成矿时代初步认为发生在晚侏罗世—早白垩世[5]。对该铜矿床的矿床地质研究表明闪长玢岩岩脉和二长斑岩岩脉/岩株侵位于古生代花岗闪长岩岩基之内，铜矿化主要产于二长斑岩岩株之上的热液角砾岩体内；钻孔揭露表明二长斑岩岩株内发育明显的钾化蚀变，可见少量黄铜矿化和辉钼矿化。以上侵位关系和矿化蚀变特征表明，斑岩侵入体与铜矿化具有明显的时空和成因联系。基于此，本文对矿区内闪长玢岩、二长斑岩进行了 U-Pb 同位素定年和元素地球化学分析，以期确定六九山铜矿床成矿作用发生的时限，为深入揭示大兴安岭地区深部岩浆动力学过程对区域大规模铜成矿作用的制约提供数据支撑。

1　成矿地质背景与矿区地质

六九山铜矿床产在黑龙江省龙江县六九村北，地处大兴安岭隆起带与松辽盆地交界带嫩江—八里罕深断裂的西侧(图 1a)。区域出露的地层主要有上古生界二叠系下统高家窝棚组、中生界龙江组和光华组，发育华力西晚期花岗闪长岩、黑云母花岗岩、碱性花岗岩和燕山晚期闪长玢岩、花岗闪长岩、花岗斑岩、二长斑岩、正长斑岩和石英斑岩等。区域构造主要是罕达罕河、宝泉子—西六九、乐业—茶壶嘴东山断裂和二龙山褶皱等[2-4]。矿床地质研究表明，矿区内出露的地质体主要是中生界光华组流纹熔岩和华力西晚期花岗闪长岩、燕山期闪长玢岩和二长斑岩等；构造以北东向和北西向断裂发育为特征，两者联合控制着该区火山机构分布，六九山矿床发育在东南侧火山口的一侧[4]。闪长玢岩和二长斑岩岩脉就位于同一构造体系，遭受了不同程度的热液蚀变；前者普遍发生青磐岩化和绢云母化，而后者受钾化和绢云母化蚀变影响，两种蚀变类型均发育在顶部高级泥化带之下；该矿区内铜成矿作用普遍发生在绢云母化带中，表明与成矿密切相关的岩浆热事件是闪长玢岩和二长斑岩。光华组流纹熔岩形成于成矿期后，不整合覆盖于矿体之上(图 1b)。矿体为超浅成盲矿体，含铜硫化物沉淀在蚀变角砾岩裂隙和隐爆角砾之间[4]。

2　样品和实验方法

实验样品采自矿区露天采场的脉状闪长玢岩和

二长斑岩,采样位置见图1b;岩相学特征详见图2和表1。锆石U-Pb定年和全岩元素分析实验方法如下。

2.1 锆石U-Pb同位素定年

锆石分离在河北省区域地质调查所实验室完成,U-Pb同位素定年在吉林大学地球科学学院实验中心完成。测试在显微镜和CL图像观察基础上进行,仪器为美国Coherent公司的Com Pex 102 Excimer Laser,ICP-MS为Agilent公司生产的Agilent 7500a激光剥蚀系统。测试采用国际标准锆石91500作为外标标准物质;数据处理采用GLITTER程序,锆石谐和图谱和加权平均年龄计算采用Isoplot程序。LA-ICP-MS分析的详细方法和流程见文献[5]。

2.2 全岩元素分析

全岩地球化学数据(主量元素和微量元素)测试实验在北京核工业分析测试中心完成。主量元素采用X荧光光谱(XRF)玻璃熔片法分析,这种方法能够分析80多种元素,其检测的质量分数范围可以从10^{-2}变化到10^{-6},分析精度优于±1%。微量和稀土元素分析采用电感耦合等离子体质谱法(ICP-MS)进行,采用BHVO-1、AVG-1和G-2等国际标准物质进行质量监控,并作空白样进行质量监控,分析精度优于±2%。具体测试方法和流程详见文献[6]。

3 实验结果

3.1 锆石U-Pb同位素定年结果

闪长玢岩(LJ222-6)锆石U-Pb同位素定年结果见表2。锆石按年龄可分为2组:第1组锆石呈短柱锥状,内部宽带结构为主,有环带结构(图3a),局部被熔化的特征显示可能为捕获锆石;大小

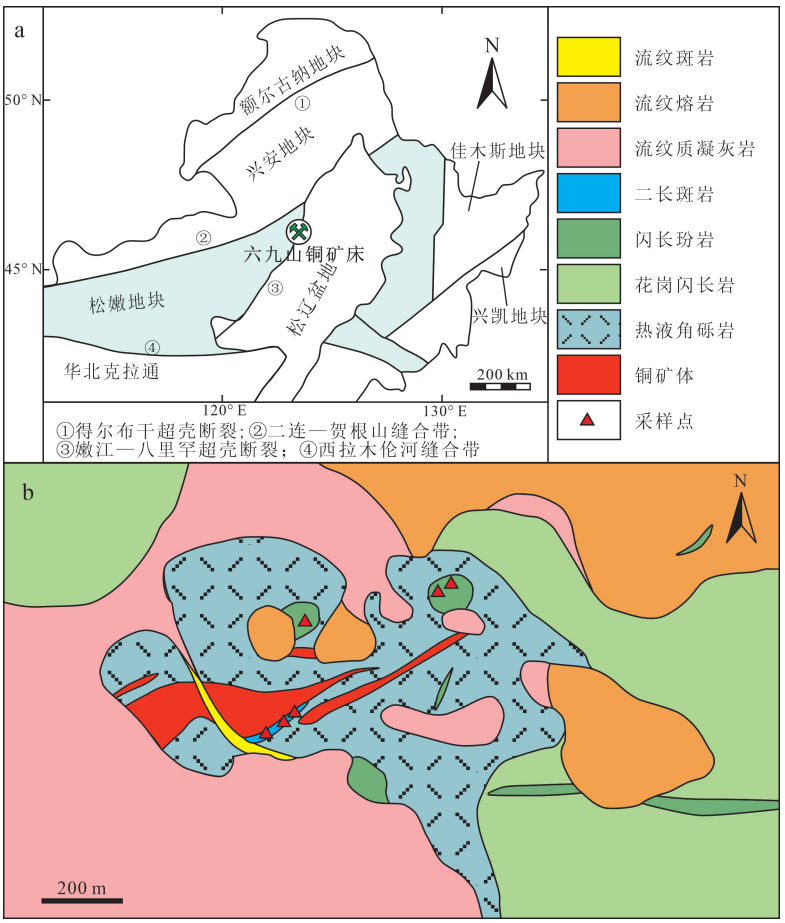

据文献[4]修编。

图1 东北地区构造分区(a)和六九山铜矿床地质简图(b)

Fig.1 Map showing the tectonic units of Northeast China (a) and geological sketch map of Liujiushan Cu deposit (b)

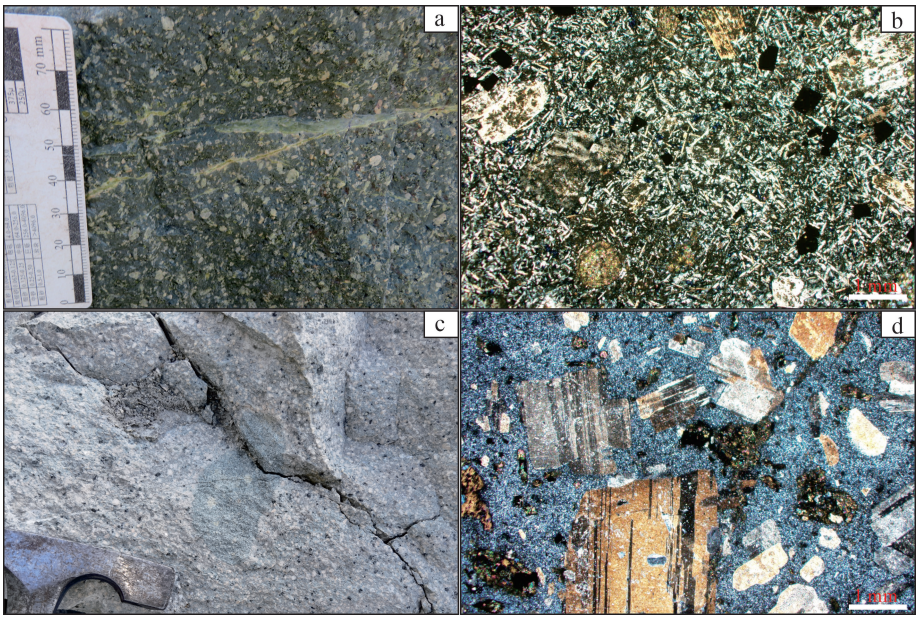

a. 闪长玢岩，斑状结构，斑晶矿物主要为角闪石和斜长石，可见热液细脉穿插；b. 闪长玢岩内角闪石矿物普遍被绿泥石取代，斜长石蚀变为绢云母，基质由微晶斜长石和角闪石组成（正交偏光）；c. 二长斑岩，斑状结构，斑晶矿物主要由斜长石、正长石和黑云母组成；d. 二长斑岩内黑云母矿物蚀变为绿泥石，长石类矿物发生较弱的绢云母化蚀变，基质发生了明显的规划蚀变（正交偏光）。

图 2　六九山铜矿床中与成矿密切相关岩石手标本和显微照片

Fig.2　Photographs and photomicrographs of Liujiushan Cu deposit

表 1　研究区样品的地质、岩相学基本特征

Table 1　Field geology and petrography of samples in the study area

岩石名称	地质产状	岩石结构	矿物组成	蚀变矿化	副矿物
闪长玢岩	脉状产出，侵入晚二叠世花岗闪长岩，走向 NE—NEE 向，北西或南东倾，倾角 70°～80°，宽 5～10 m	块状构造，斑状结构，基质为交织结构	斑晶体积分数为 5%～7%，斜长石为主，少量黑云母、角闪石、辉石等。基质为斜长石、钾长石微晶，隐晶质矿物	绿帘石、钠长石、高岭土化以及黄铁矿化	磁铁矿、锆石、磷灰石等
二长斑岩	脉状/岩株状产出，侵入晚二叠世花岗闪长岩，内部可见浑圆状闪长质微粒包体；走向 NE 向，北西或南东倾，倾角 75°～85°，宽 15～20 m	块状构造，斑状结构，基质为细晶、隐晶质结构	斑晶体积分数约为 30%，斜长石为主，少量正长石、角闪石、黑云母以及石英。基质为细晶、隐晶质长英质矿物	绿帘石、方解石、高岭土化等	磁铁矿、锆石、磷灰石、榍石等

为 50 μm×60 μm～80 μm×100 μm，长宽比为 1∶1～1.5∶1，w(Th)为 39.09×10^{-6}～132.70×10^{-6}，w(U)为 58.92×10^{-6}～320.76×10^{-6}，Th/U 值为 0.41～0.91，整体呈现岩浆锆石属性[7]；获得加权平均年龄为（294.9±4.2）Ma（n=8，MSWD=0.08，表 2）。鉴于这组锆石与前人所定绢英岩的锆石 U-Pb 定年一致[7]，其年龄应为赋矿围岩晚古生代花岗闪长岩就位年龄，应为捕获锆石。第 2 组锆石特征自形板状，环带结构发育（图 3a），大小为 40 μm×50 μm～50 μm×100 μm，长宽比为 1∶1～2∶1，w(Th)为 103.38×10^{-6}～530.15×10^{-6}，w(U)为 110.40×10^{-6}～590.94×10^{-6}，Th/U 值为 0.77～1.38；获得锆石的^{206}Pb/^{238}U 同位素年龄为 134.9～126.0 Ma（表 2、图 3b），加权平均年龄为（132.6±2.6）Ma（n=5，MSWD=1.2，图 3b），进而厘定闪长玢岩岩浆就位发生在中生代早白垩世。

表 2 六九山铜矿床闪长玢岩和二长斑岩 LA－ICP－MS 锆石 U－Pb 同位素定年结果

Table 2 LA－ICP－MS zircon U－Pb age data of diorite porphyry and monzonite porphyry in Liujiushan Cu deposit

岩性	测点号	$w_B/10^{-6}$			Th/U	同位素比值						年龄/Ma					
		Pb	Th	U		$^{207}Pb/^{206}Pb$	σ	$^{207}Pb/^{235}U$	σ	$^{206}Pb/^{238}U$	σ	$^{207}Pb/^{206}Pb$	σ	$^{206}Pb/^{238}U$	σ	$^{207}Pb/^{235}U$	σ
闪长玢岩	LJ222－6－1	2.76	106.02	127.96	0.83	0.054 45	0.004 19	0.349 37	0.026 23	0.046 53	0.001 09	389.8	164.3	293.2	6.7	304.2	19.7
	LJ222－6－4	1.93	72.33	80.19	0.90	0.055 25	0.004 32	0.362 25	0.027 59	0.047 55	0.001 13	422.3	165.8	299.4	6.9	313.9	20.6
	LJ222－6－5	2.71	100.40	110.42	0.91	0.052 46	0.003 02	0.338 24	0.019 10	0.046 76	0.000 88	305.3	125.9	294.6	5.4	295.8	14.5
	LJ222－6－8	0.99	39.09	58.92	0.66	0.052 16	0.004 41	0.334 51	0.027 60	0.046 51	0.001 14	292.4	181.7	293.1	7.0	293.0	21.0
	LJ222－6－9	1.82	63.74	96.58	0.66	0.054 46	0.003 56	0.351 93	0.022 49	0.046 86	0.000 96	390.3	139.9	295.2	5.9	306.2	16.9
	LJ222－6－13	1.27	46.66	66.18	0.71	0.057 83	0.003 70	0.373 19	0.023 30	0.046 80	0.000 98	523.3	134.8	294.8	6.0	322.0	17.2
	LJ222－6－15	5.31	132.70	320.76	0.41	0.055 99	0.002 41	0.361 15	0.015 30	0.046 78	0.000 78	451.6	93.1	294.7	4.8	313.1	11.4
	LJ222－6－18	1.04	39.93	68.63	0.58	0.052 64	0.003 98	0.339 88	0.025 08	0.046 83	0.001 06	313.1	162.7	295.0	6.5	297.1	19.0
	LJ222－6－20	6.51	530.15	590.94	0.90	0.052 17	0.002 19	0.152 08	0.006 30	0.021 14	0.000 34	293.0	93.1	134.9	2.2	143.7	5.6
	LJ222－6－19	1.28	103.38	110.40	0.94	0.055 20	0.005 48	0.158 98	0.015 31	0.020 89	0.000 60	420.3	207.8	133.3	3.8	149.8	13.4
	LJ222－6－3	2.84	233.14	303.80	0.77	0.049 44	0.004 15	0.139 07	0.011 37	0.020 40	0.000 49	168.5	184.9	130.2	3.1	132.2	10.1
	LJ222－6－6	5.74	440.01	317.97	1.38	0.049 37	0.004 32	0.142 86	0.012 18	0.020 99	0.000 52	165.4	192.5	133.9	3.3	135.6	10.8
	LJ222－6－7	2.16	183.30	194.27	0.94	0.050 19	0.005 76	0.136 60	0.015 25	0.019 74	0.000 62	203.9	246.3	126.0	3.9	130.0	13.6
二长斑岩	LJ－3－1	4.22	366.76	310.97	1.18	0.048 89	0.003 84	0.142 22	0.010 90	0.021 09	0.000 49	142.5	174.7	134.5	3.1	135.0	9.7
	LJ－3－2	1.42	119.99	176.90	0.68	0.048 96	0.005 28	0.146 10	0.015 35	0.021 63	0.000 63	145.8	235.0	138.0	4.0	138.5	13.6
	LJ－3－3	3.75	334.22	266.20	1.26	0.048 92	0.005 28	0.145 91	0.015 31	0.021 62	0.000 65	144.2	235.2	137.9	4.1	138.3	13.6
	LJ－3－4	3.97	352.26	288.97	1.22	0.049 39	0.003 43	0.142 63	0.009 66	0.020 93	0.000 44	166.6	154.5	133.6	2.8	135.4	8.6
	LJ－3－5	2.20	179.13	193.21	0.93	0.048 98	0.003 83	0.141 15	0.010 77	0.020 89	0.000 47	146.9	173.7	133.3	3.0	134.1	9.6
	LJ－3－6	2.23	189.68	232.17	0.82	0.048 77	0.003 70	0.137 69	0.010 19	0.020 47	0.000 46	137.0	169.1	130.6	2.9	131.0	9.1
	LJ－3－8	1.89	176.49	171.36	1.03	0.049 60	0.005 18	0.141 96	0.014 44	0.020 75	0.000 58	176.4	226.8	132.4	3.7	134.8	12.8
	LJ－3－9	2.15	177.28	216.78	0.82	0.048 70	0.004 75	0.139 29	0.013 25	0.020 74	0.000 56	133.3	214.6	132.3	3.5	132.4	11.8
	LJ－3－10	2.02	184.49	190.30	0.97	0.048 76	0.004 46	0.136 06	0.012 15	0.020 24	0.000 51	136.2	202.0	129.1	3.2	129.5	10.9
	LJ－3－11	2.10	174.78	188.22	0.93	0.048 87	0.004 54	0.140 59	0.012 73	0.020 87	0.000 55	141.5	204.8	133.1	3.5	133.6	11.3
	LJ－3－12	1.56	130.99	158.60	0.83	0.048 70	0.003 60	0.139 17	0.010 06	0.020 73	0.000 44	133.5	165.2	132.2	2.8	132.3	9.0
	LJ－3－13	1.98	161.46	160.55	1.01	0.049 13	0.005 31	0.135 88	0.014 28	0.020 06	0.000 59	154.0	235.3	128.0	3.8	129.4	12.8
	LJ－3－14	4.73	417.18	333.03	1.25	0.049 15	0.004 27	0.142 46	0.012 05	0.021 02	0.000 52	154.9	191.6	134.1	3.3	135.2	10.7

续表 2

岩性	测点号	$w_B/10^{-6}$			Th/U	同位素比值						年龄/Ma					
		Pb	Th	U		$^{207}Pb/^{206}Pb$	σ	$^{207}Pb/^{235}U$	σ	$^{206}Pb/^{238}U$	σ	$^{207}Pb/^{206}Pb$	σ	$^{206}Pb/^{238}U$	σ	$^{207}Pb/^{235}U$	σ
二长斑岩	LJ-3-16	2.08	172.94	230.03	0.75	0.050 37	0.004 75	0.144 52	0.013 27	0.020 81	0.000 55	212.3	204.9	132.8	3.5	137.1	11.8
	LJ-3-17	2.67	218.59	218.62	1.00	0.050 00	0.004 07	0.141 03	0.011 18	0.020 46	0.000 48	195.2	178.9	130.6	3.1	134.0	10.0
	LJ-3-18	2.83	252.35	314.34	0.80	0.049 44	0.002 79	0.143 49	0.007 92	0.021 06	0.000 39	168.5	126.6	134.3	2.4	136.1	7.0
	LJ-3-19	3.50	309.78	289.80	1.07	0.048 84	0.004 82	0.138 28	0.013 29	0.020 54	0.000 56	140.4	216.6	131.1	3.5	131.5	11.9
	LJ-3-20	3.28	295.99	234.37	1.26	0.048 84	0.006 73	0.140 99	0.018 90	0.020 95	0.000 74	140.2	294.6	133.6	4.7	133.9	16.8
	LJ-3-21	2.53	219.79	247.92	0.89	0.048 68	0.002 97	0.136 87	0.008 16	0.020 41	0.000 39	132.3	137.4	130.2	2.5	130.3	7.3
	LJ-3-22	1.57	130.40	162.96	0.80	0.049 23	0.003 84	0.142 04	0.010 81	0.020 94	0.000 47	158.7	172.9	133.6	3.0	134.9	9.6
	LJ-3-23	3.27	286.38	237.10	1.21	0.048 54	0.004 50	0.135 11	0.012 19	0.020 20	0.000 52	125.5	204.6	128.9	3.3	128.7	10.9
	LJ-3-24	1.99	173.97	248.25	0.70	0.049 49	0.002 93	0.140 50	0.008 13	0.020 61	0.000 39	171.3	132.6	131.5	2.5	133.5	7.2

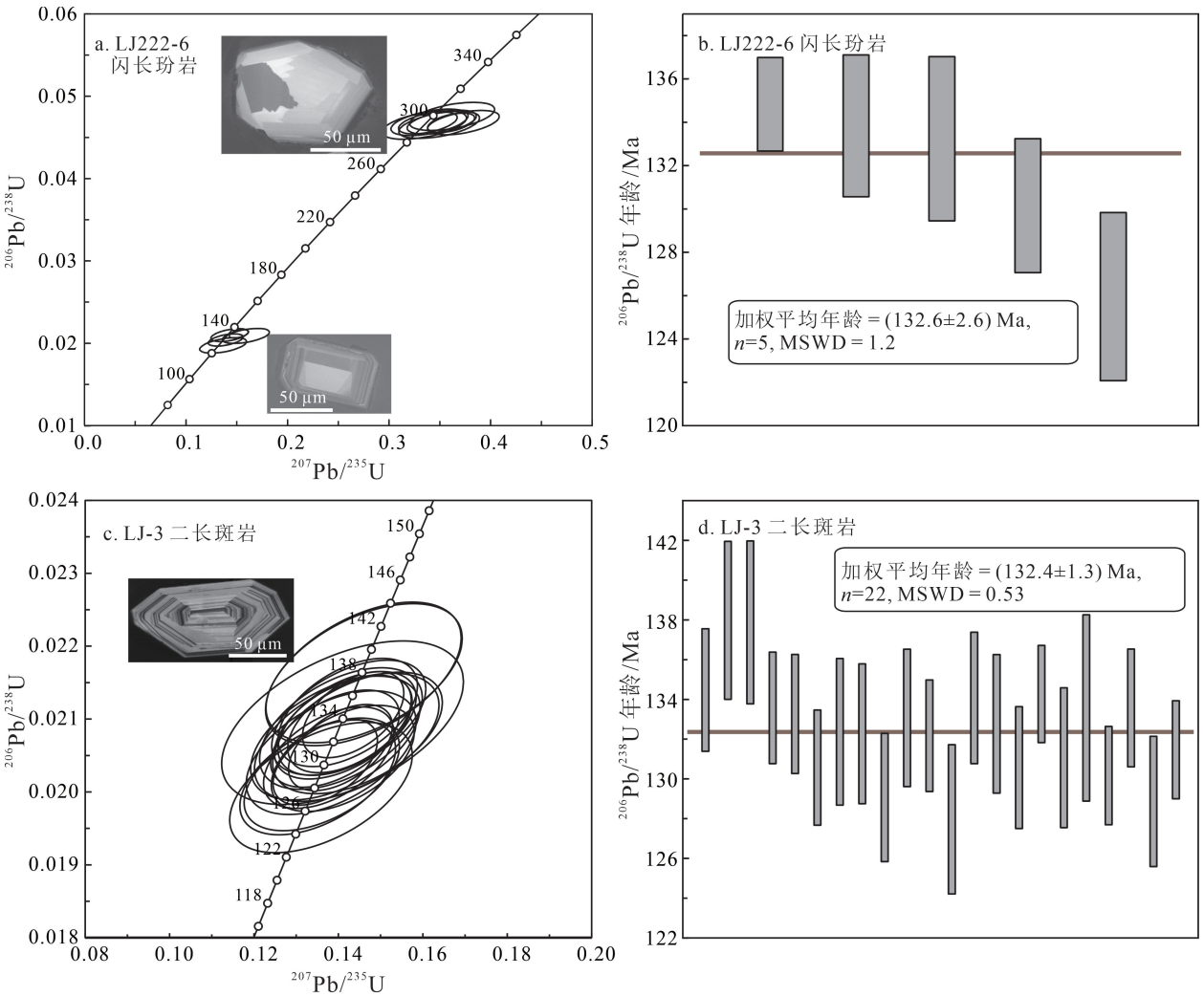

图3 研究区锆石U-Pb同位素定年谐和图(a, c)和加权平均年龄图(b, d)

Fig.3 Zircon U-Pb concordia diagram (a, c) and weighted average age (b, d) in the study area

二长斑岩(LJ-3)锆石CL图像显示,其晶形多呈短柱锥状,少数呈长柱锥状,大小介于50 μm×50 μm~70 μm×120 μm之间,长宽比为1∶1~3∶1(图3c),内部发育韵律环带,w(Th)为119.99×10^{-6}~417.18×10^{-6},w(U)为158.60×10^{-6}~333.03×10^{-6},Th/U值为0.68~1.26,为浅成岩浆就位结晶的产物[8]。22粒锆石U-Pb同位素定年结果见表2,获得$^{206}Pb/^{238}U$年龄在138.0~128.0 Ma之间(图3c),加权平均年龄为(132.4±1.3)Ma(n=22,MSWD=0.53;图3d),进而厘定二长斑岩岩浆就位发生在中生代早白垩世。

3.2 元素地球化学特征

3.2.1 闪长玢岩

元素地球化学测试结果见表3。由表3可知,闪长玢岩的w(SiO_2)为52.98%~59.83%,w(Al_2O_3)为16.57%~19.46%,w(Fe_2O_3)为5.80%~7.78%,w(FeO)为3.16%~3.45%,w(MgO)为2.50%~2.60%,w(CaO)为3.41%~5.90%,w(K_2O)为2.86%~3.91%,w(Na_2O)为2.99%~4.85%,w(TiO_2)为0.83%~1.20%,w(P_2O_5)为0.26%~0.37%,w(Na_2O+K_2O)为6.90%~8.04%,Na_2O/K_2O值为0.76~1.67,镁指数($Mg^{\#}$=w(MgO)/40/(w(MgO)/40+0.8998w(TFe_2O_3)/72))为0.67~0.71;表明岩石整体属于中基性岩浆岩特征。在TAS分类图解(图4a)上成分点落在二长闪长岩区域和二长岩区域,在w(K_2O)-w(SiO_2)岩石系列分类图解(图4b)上样品成分点落在钾玄岩系列区域。这种特征表明其为碱质、中基性钾玄岩系列岩浆。

表 3　六九山铜矿床闪长玢岩和二长斑岩主量元素和微量元素组成

Table 3　Major- and trace-element concentrations of diorite porphyry and monzonite porphyry in Liujiushan Cu deposit

样品号	岩石名称	SiO_2	Al_2O_3	Fe_2O_3	FeO	MgO	CaO	Na_2O	K_2O	MnO	TiO_2	P_2O_5	烧失量	总和	Na_2O+K_2O	Na_2O/K_2O	Fe_2O_3/FeO	$Mg^{\#}$
LJ-2-1	闪长玢岩	54.27	18.82	7.78	3.18	2.54	4.93	4.85	3.19	0.12	1.20	0.37	1.52	99.60	8.04	1.52	2.45	0.67
LJ-2-2	闪长玢岩	59.83	16.57	5.80	3.45	2.60	3.41	2.99	3.91	0.09	0.83	0.26	3.34	99.63	6.90	0.76	1.68	0.71
LJ-2-3	闪长玢岩	52.98	19.46	7.61	3.16	2.50	5.90	4.77	2.86	0.11	1.17	0.36	1.88	99.60	7.63	1.67	2.41	0.69
LJ-3-1	二长斑岩	66.90	15.57	3.36	1.90	1.32	2.09	5.82	2.70	0.09	0.52	0.18	1.01	99.55	8.52	2.16	1.77	0.19
LJ-3-2	二长斑岩	67.22	15.35	3.43	1.77	1.25	2.38	5.86	2.49	0.08	0.51	0.16	0.83	99.56	8.35	2.35	1.94	0.21
LJ-3-3	二长斑岩	67.56	15.33	3.41	1.87	1.25	2.35	5.64	2.44	0.08	0.53	0.17	0.82	99.58	8.08	2.31	1.82	0.18

样品号	岩石名称	Li	Be	Rb	Sr	Cs	Ba	Th	U	Nb	Ta	Zr	Hf	Rb/Sr	Nb/Ta	Th/U	Zr/Hf	La	Ce
LJ-2-1	闪长玢岩	27.00	1.82	80.60	748.00	1.30	984.00	1.80	0.67	4.79	0.31	205.00	4.48	0.11	15.30	2.67	45.76	19.70	40.00
LJ-2-2	闪长玢岩	31.40	1.80	88.10	363.00	3.10	786.00	6.21	1.46	6.67	0.49	249.00	6.75	0.24	13.67	4.25	36.89	27.70	49.20
LJ-2-3	闪长玢岩	26.50	1.84	71.60	802.00	1.88	823.00	1.64	0.60	4.59	0.30	168.00	4.40	0.09	15.56	2.72	38.18	18.90	39.50
LJ-3-1	二长斑岩	11.30	1.78	60.10	590.00	0.74	922.00	4.47	1.58	3.90	0.30	118.00	3.80	0.10	12.96	2.83	31.05	19.90	37.60
LJ-3-2	二长斑岩	13.90	1.83	56.10	488.00	0.91	866.00	4.46	2.40	3.79	0.31	119.00	3.59	0.11	12.11	1.86	33.15	19.60	38.40
LJ-3-3	二长斑岩	11.50	1.91	53.80	525.00	0.74	857.00	4.59	1.47	3.89	0.29	119.00	3.59	0.10	13.32	3.12	33.15	20.30	36.70

样品号	岩石名称	Pr	Nd	Sm	Eu	Gd	Tb	Dy	Ho	Er	Tm	Yb	Lu	Y	ΣREE	LREE/HREE	$(La/Yb)_N$	Sm/Nd	δEu
LJ-2-1	闪长玢岩	5.57	26.30	5.71	1.49	4.07	0.71	3.65	0.71	2.06	0.30	1.92	0.29	18.90	112.48	7.20	7.36	0.22	0.54
LJ-2-2	闪长玢岩	6.31	26.80	5.60	1.03	3.89	0.66	3.57	0.67	1.87	0.28	1.85	0.28	16.80	129.70	8.93	10.74	0.21	0.39
LJ-2-3	闪长玢岩	5.44	24.80	5.43	1.49	3.92	0.72	3.73	0.72	1.86	0.29	1.73	0.28	18.90	108.81	7.21	7.84	0.22	0.57
LJ-3-1	二长斑岩	4.53	18.00	3.08	0.74	2.37	0.33	1.57	0.26	0.75	0.10	0.68	0.10	6.95	90.01	13.61	20.96	0.17	0.49
LJ-3-2	二长斑岩	4.24	16.40	3.20	0.84	2.40	0.38	1.71	0.27	0.77	0.12	0.68	0.11	7.36	89.11	12.85	20.77	0.20	0.54
LJ-3-3	二长斑岩	4.46	18.20	3.44	0.81	2.49	0.38	1.82	0.30	0.79	0.11	0.69	0.10	7.97	90.58	12.58	21.23	0.19	0.49

注：主量元素质量分数单位为%；微量和稀土元素质量分数单位为 10^{-6}。

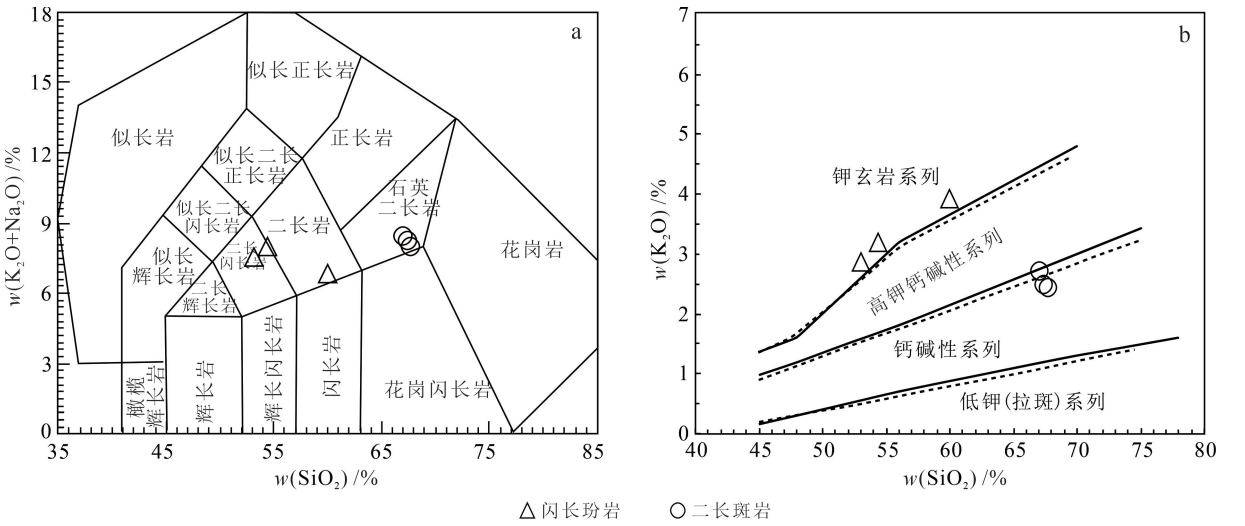

图a底图据文献[9];图b底图据文献[10]。

图4 六九山铜矿床浅成侵入岩岩石化学TAS图解(a)和岩石化学$w(K_2O)$-$w(SiO_2)$岩系图解(b)

Fig.4 $w(K_2O+Na_2O)$ versus $w(SiO_2)$ plot (a) and $w(K_2O)$ versus $w(SiO_2)$ plot (b) of hypabyssal intrusive rocks in Liujiushan Cu deposit

在微量和稀土元素方面,闪长玢岩明显富集大离子亲石元素(LILE),$w(Li)$为$26.50\times10^{-6}\sim31.40\times10^{-6}$,$w(Cs)$为$1.30\times10^{-6}\sim3.10\times10^{-6}$,$w(Ba)$为$786.00\times10^{-6}\sim984.00\times10^{-6}$,$w(Rb)$为$71.60\times10^{-6}\sim88.10\times10^{-6}$;相对亏损高场强元素(HFSE),$w(Th)$为$1.64\times10^{-6}\sim6.21\times10^{-6}$,$w(U)$为$0.60\times10^{-6}\sim1.46\times10^{-6}$,$w(Nb)$为$4.59\times10^{-6}\sim6.67\times10^{-6}$,$w(Ta)$为$0.30\times10^{-6}\sim0.49\times10^{-6}$,$w(Zr)$为$168.00\times10^{-6}\sim249.00\times10^{-6}$,$w(Hf)$为$4.40\times10^{-6}\sim6.75\times10^{-6}$,$w(Y)$为$16.80\times10^{-6}\sim18.90\times10^{-6}$;$w(\sum REE)$为$108.81\times10^{-6}\sim129.70\times10^{-6}$,LREE/HREE值为7.20~8.93,$(La/Yb)_N$为7.36~10.74,Sm/Nd值为0.21~0.22,δEu为0.39~0.57。在原始地幔标准化图谱(图5a)上,呈现明显富集大离子亲石元素(Cs、Rb、Ba、K等),相对亏损高场强元素Th、U、Nb、Ta等特征;在稀土元素的球粒陨石标准化图解(图5b)上,呈现中等分馏右倾斜、Eu异常不明显或弱的负异常特征。以上特征表明该类岩石具有典型岛弧岩浆的地球化学特征[13-14]。Nb和Ta元素的亏损暗示岩浆来源于地壳或受到地壳物质的强烈混染,具有与板块俯冲作用有关的岛弧、大陆边缘岩浆弧的岩浆属性[15-16];弱的Eu异常特征反映岩浆演化过程中斜长石分离结晶或源区残留较少。

3.2.2 二长斑岩

从表3可知,二长斑岩的$w(SiO_2)$为66.90%~67.56%,$w(Al_2O_3)$为15.33%~15.57%,$w(Fe_2O_3)$为3.36%~3.43%,$w(FeO)$为1.77%~1.90%,$w(MgO)$为1.25%~1.32%,$w(CaO)$为2.09%~2.38%,$w(K_2O)$为2.44%~2.70%,$w(Na_2O)$为5.64%~5.86%,$w(TiO_2)$为0.51%~0.53%,$w(P_2O_5)$为0.16%~0.18%,$w(K_2O+Na_2O)$为8.08%~8.52%,Na_2O/K_2O值为2.16~2.35,$Mg^{\#}$为0.18~0.21;表明其属于中酸性岩浆岩范畴。在TAS图解(图4a)上,成分点均落在石英二长岩区域,在$w(K_2O)$-$w(SiO_2)$岩石系列分类图解(图4b)上,成分点落在高钾钙碱性系列与钙碱性岩系列分界线区域;较高的Na_2O/K_2O值指示其为碱性、钠质中酸性、高钾钙碱性岩系与钙碱性岩系过渡岩系。

在微量元素方面,其富集大离子亲石元素(LILE),$w(Li)$为$11.30\times10^{-6}\sim13.90\times10^{-6}$,$w(Cs)$为$0.74\times10^{-6}\sim0.91\times10^{-6}$,$w(Ba)$为$857.00\times10^{-6}\sim922.00\times10^{-6}$,$w(Rb)$为$53.80\times10^{-6}\sim60.10\times10^{-6}$;相对亏损高场强元素(HFSE),$w(Th)$为$4.46\times10^{-6}\sim4.59\times10^{-6}$,$w(U)$为$1.47\times10^{-6}\sim2.40\times10^{-6}$,$w(Nb)$为$3.79\times10^{-6}\sim3.90\times10^{-6}$,$w(Ta)$为$0.29\times10^{-6}\sim0.31\times10^{-6}$,$w(Zr)$为$118.00\times10^{-6}\sim119.00\times10^{-6}$,$w(Hf)$为$3.59\times10^{-6}\sim3.80\times10^{-6}$,$w(Y)$为$6.95\times10^{-6}\sim7.97\times10^{-6}$;稀土元素$w(\sum REE)$为$89.11\times10^{-6}\sim90.58\times$

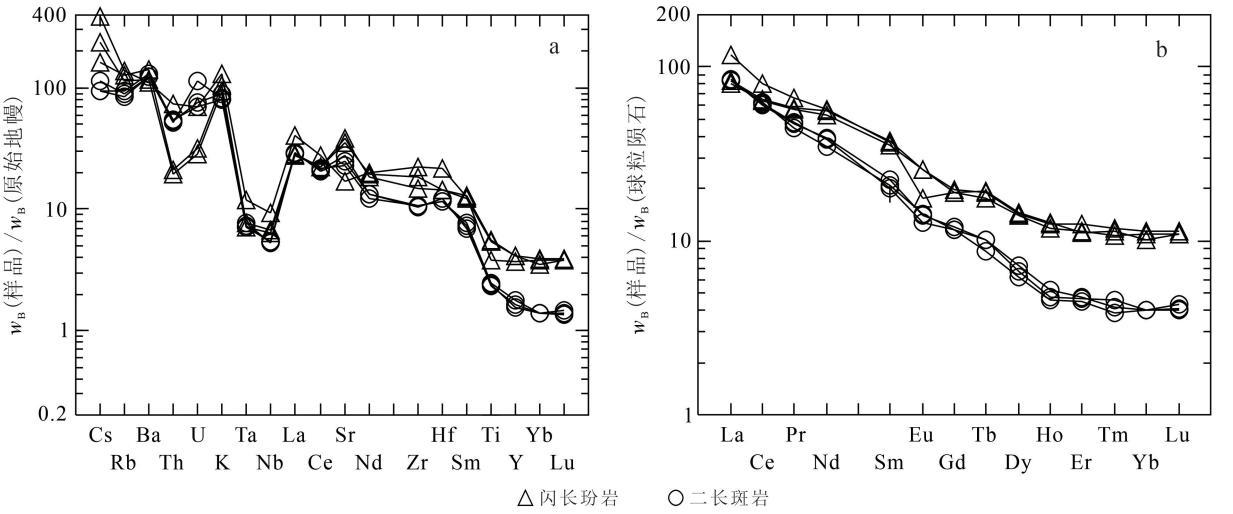

原始地幔标准化数值据文献[11];球粒陨石标准化数值据文献[12]。

图 5　六九山铜矿床侵入岩原始地幔标准化微量元素蛛网图解(a)和球粒陨石标准化稀土元素配分图解(b)

Fig.5　Primitive mantle-normalized trace element patterns (a) and chondrite-normalized REE patterns (b) of intrusive rocks in Liujiushan Cu deposit

10^{-6},LREE/HREE 值为 12.58～13.61,$(La/Yb)_N$ 为 20.77～21.23,Sm/Nd 值为 0.17～0.20,δEu 为 0.49～0.54。在原始地幔标准化图谱(图 5a)上,呈现明显富集大离子亲石元素(Cs、Rb、Ba、K 等),明显亏损高场强元素 Nb、Ta 和相对亏损 Th、Ti、Y、Yb、Lu 等高场强元素特征;在球粒陨石标准化图解(图 5b)上,呈现中等分馏右倾、Eu 异常不明显特征;以上特征表明该类岩石具有典型岛弧岩浆的地球化学特征[13-14]。Nb 和 Ta 元素的亏损暗示岩浆来源于地壳或是受到地壳物质的强烈混染,可能与板块俯冲作用有关[15-16];Eu 异常不明显的特征反映岩浆演化过程中斜长石分离结晶或源区残留相对有限。

4　讨论

4.1　成岩成矿时代和地质意义

如前所述,六九山铜矿床产在大兴安岭隆起带与松辽盆地交界带嫩江—八里罕深断裂的西侧或大兴安岭东坡中北段(图 1a),区域铜成矿系统与成矿密切的岩浆作用时代研究表明,富克山、小科勒河斑岩铜矿成矿系统的花岗闪长斑岩、花岗斑岩形成年龄分别为(152.5±1.7)Ma、(150.0±1.6)Ma[17],布敦花斑岩-浅成热液铜多金属成矿系统的花岗闪长斑岩形成年龄为(151.7±1.3)Ma,闹牛山浅成热液高硫化型铜矿床的花岗闪长斑岩形成时代为(141.2±0.7)Ma[18]。本次获得闪长玢岩岩浆结晶于(132.6±2.6)Ma,二长斑岩就位于(132.4 ± 1.3)Ma,二者应为深部岩浆房在不同演化阶段的产物;鉴于闪长玢岩和二长斑岩结晶年龄与获得的矿石矿物辉钼矿 Re-Os 同位素年龄相符((134.1±0.8)Ma,成果待发表),揭示六九山铜成矿作用与早白垩世岩浆就位有密切的时空联系。这些精确的地质年代学数据结果限定六九山铜成矿作用过程持续时间小于 1 Ma,与全球绝大多数的斑岩成矿系统一致[19-20]。

大兴安岭地区发育有大量的不同类型的热液金属矿床,产出了大量的铜、钼、铅、锌和银以及少量的钨、锡和铁等工业金属。矿床成因类型主要包括浅成热液型、斑岩型和矽卡岩型矿床,这些矿床主要形成于 155 ～ 130 Ma(图 6)(数据来源于文献[21-47]),个别矿床形成较早,如多宝山斑岩铜钼矿床(约 480 Ma)[48] 和八大关斑岩铜钼矿床(约 230 Ma)[49]。整体而言,六九山铜矿床是大兴安岭地区早白垩世期间大规模岩浆-热液活动的产物。在矿产勘查潜力方面,六九山铜矿床顶部发育有高级泥化带,代表了典型的斑岩铜成矿系统的岩帽或顶部,表明该矿床保存程度较高,亦或遭受了较弱的成矿后剥蚀作用;结合区域上相邻的闹牛山浅成热液

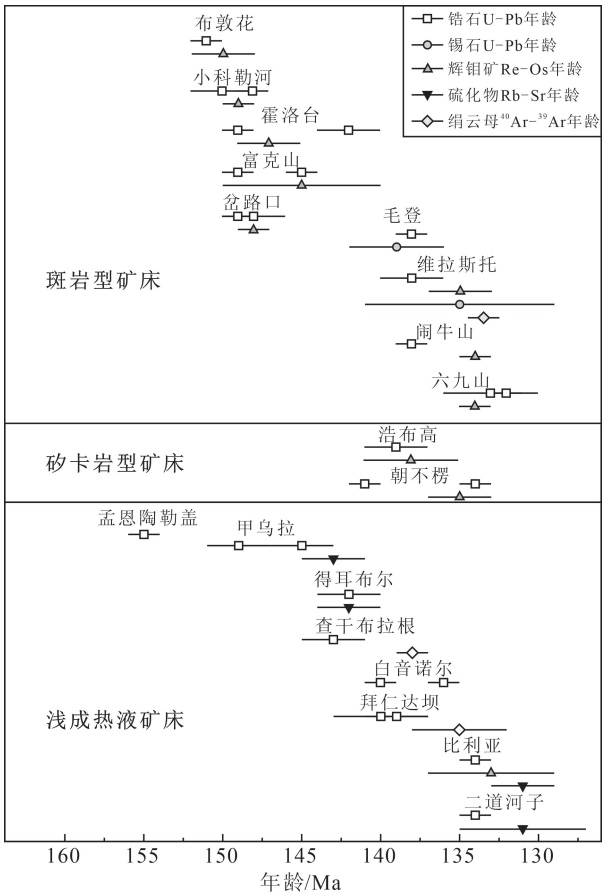

布敦花数据据文献[21-22];小科勒河数据据文献[23-24];霍洛台数据据文献[25];富克山数据据文献[26-27];岔路口数据据文献[28];毛登数据据文献[29];维拉斯托数据据文献[30-32];闹牛山数据据文献[33];浩布高数据据文献[34];朝不楞数据据文献[35-36];孟恩陶勒盖数据据文献[37];甲乌拉数据据文献[38-39];得耳布尔数据据文献[40-42];查干布拉根数据据文献[43];白音诺尔数据据文献[44];拜仁达坝数据据文献[31];比利亚数据据文献[45];二道河子数据据文献[46-47]。

图6 大兴安岭地区中生代岩浆热液型矿床地质年代学图谱

Fig.6 Summary of age data of Mesozoic magmatic-hydrothermal ore deposits in the Great Hinggan Range

铜矿床[18],表明大兴安岭中部在早白垩世后期遭受了较弱的抬升剥蚀作用,该区域有着优越的找寻相似热液金属矿床的潜力。

4.2 岩石成因类型与岩浆起源

目前,有关花岗岩的岩石成因已有多种论述,主流观点是岩石成因分类,即M型、I型、S型和A型[50-53]。上述与成矿密切相关的闪长玢岩和二长斑岩地质、岩相学和元素地球化学特征论述表明,它们均为浅成脉岩,其长英质矿物为斜长石/钠长石+正长石+石英,暗色矿物黑云母、普通角闪石、普通辉石等,副矿物有磷灰石、锆石、磁铁矿等,表明其岩石成因类型应为I型花岗岩类。微量元素地球化学特征揭示其具有典型的岛弧、大陆边缘火山弧的岩浆特征,说明它们可能为典型岛弧钙碱性或埃达克质岩浆属性(图7a)[13];在$(La/Yb)_N-(Yb)_N$和Sr/Y-w(Y)划分判别图解(图7a、b)上,闪长玢岩成分点落在岛弧钙碱性岩区,而二长斑岩成分点落在埃达克质岩区,前者具有岛弧、大陆边缘钙碱性岩属性,而后者在SiO_2、Al_2O_3、MgO、K_2O/Na_2O、Rb、Sr、Y、Yb、Sr/Y、$(La/Yb)_N$和δEu等方面均满足与大洋板块俯冲有关的埃达克岩特征。在与板块俯冲作用有关的Th/Yb-Ta/Yb岩浆源区构造判别图解(图7c)上,闪长玢岩2件成分点明显落在与大洋板块俯冲有关的富集地幔源区,闪长玢岩1件和二长斑岩成分点落在活动陆缘区域;在Rb/Y-Nb/Y图解(图7d)上,闪长玢岩、二长斑岩成分点均落在大洋俯冲提供流体交代下地壳而形成的富集地幔源区。

4.3 形成环境与地球动力学背景

如前所述,六九山铜矿床产在兴蒙造山带东部、大兴安岭东坡中北段,区域先后经历古亚洲洋构造体系和古太平洋构造体系演化。前人研究表明,古生代受古亚洲洋构造体系的控制[54-58],古亚洲洋最终闭合于晚二叠世—早三叠世期间(约250 Ma),中三叠世期间进入鄂霍茨克洋和古太平洋俯冲体系[59-60];目前,有关环太平洋构造体系开始的时间虽有争论,但众多学者认为古太平洋板块在晚三叠世晚期—早侏罗世早期开始向欧亚大陆的俯冲作用[61-64]。

六九山铜矿床成矿系统的闪长玢岩、二长斑岩锆石U-Pb同位素定年结果表明岩浆作用发生在132 Ma,成矿与斑岩岩浆就位过程具有明显的时空关系;这种特征表明成岩成矿作用发生在中生代早白垩世,其成岩成矿应形成于古太平洋板块俯冲大陆边缘岩浆弧环境。在w(Nb)-w(Y)、w(Rb)-w(Y+Nb)(图8a、b)构造环境判别图中,成分点均落在同碰撞火山弧区(图8a)和火山弧区(图8b),表明成岩成矿作用发生在碰撞与造山后火山弧阶段;这一点与区域孔雀山、莲花山和闹牛山等浅成热液铜矿床以及金鸡岭、富克山和小科勒河等斑岩型铜矿床,特别是莲花山、闹牛山等浅成热液铜矿床处于相同的构造背景[17],成岩成矿适值中生代早白垩世库拉板块向欧亚板块俯冲的大陆边缘岩浆弧背景。

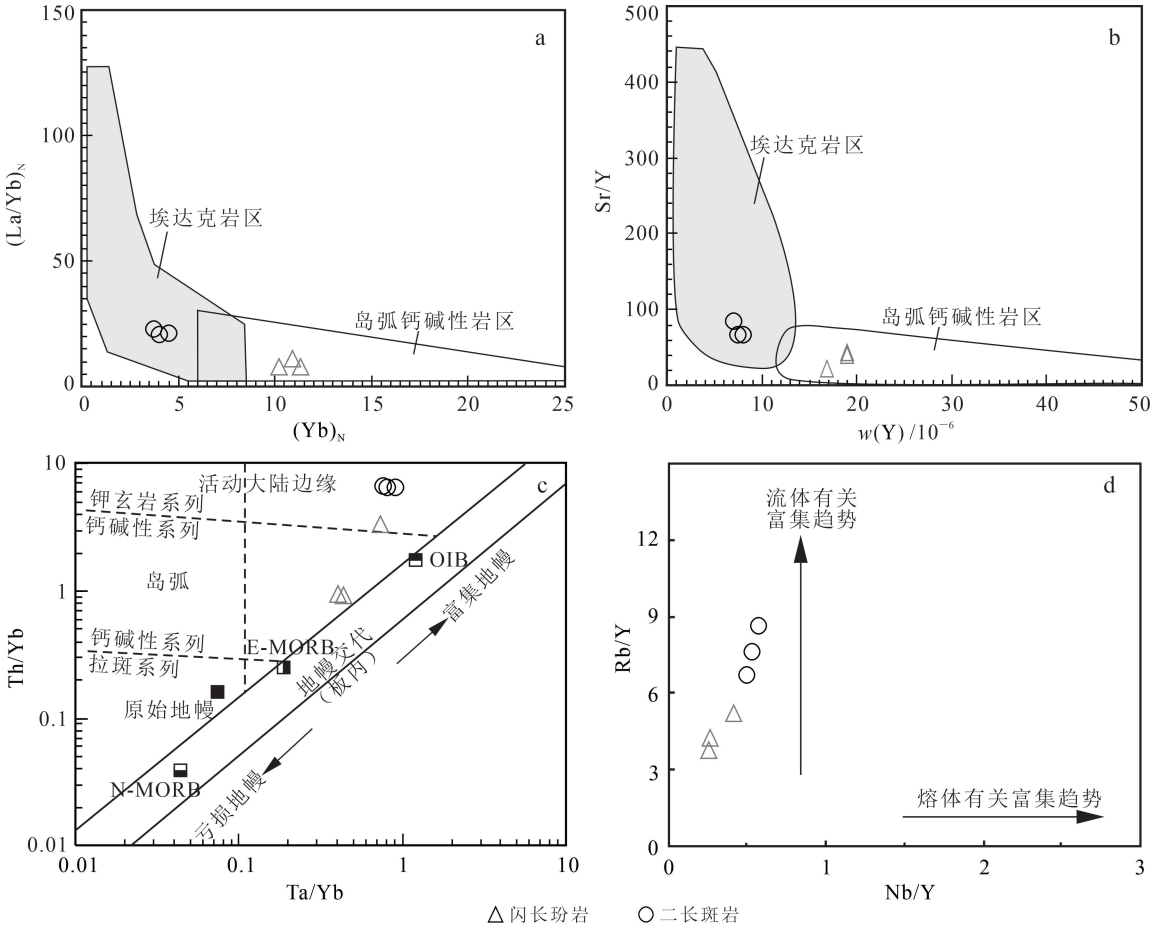

a. $(La/Yb)_N$-$(Yb)_N$成因图解;b. Sr/Y - w(Y)成因图解;c. Th/Yb - Ta/Yb 成因图解;d. Rb/Y - Nb/Y 成因图解。OIB.洋岛玄武岩;E - MORB.富集洋中脊玄武岩;N - MORB.正常洋中脊玄武岩。

图 7　研究区闪长玢岩和二长斑岩元素比值岩石成因类型图解

Fig.7　Petrogenesis diagrams of elemental ratios of diorite porphyry and monzonite porphyry in the study area

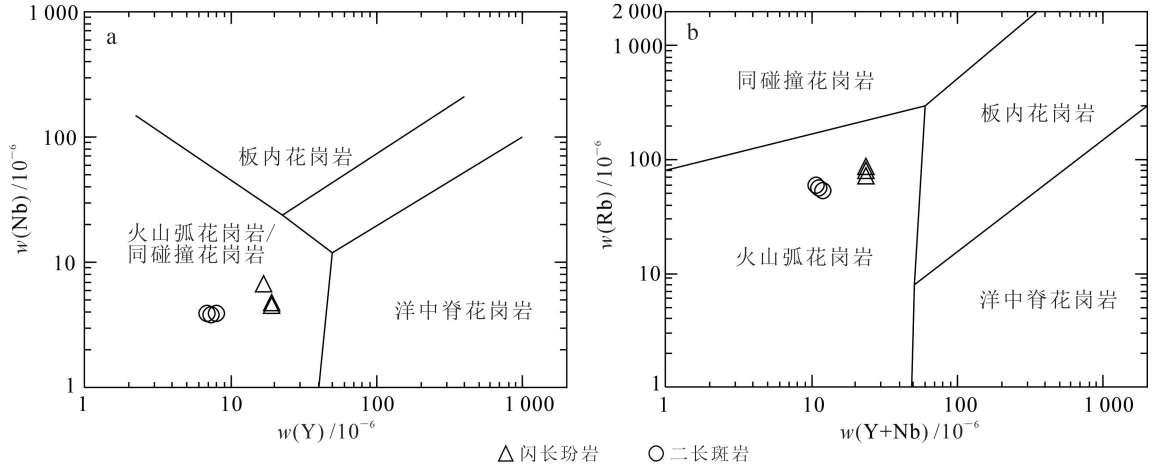

底图据文献[54, 65]。

图 8　六九山铜矿床闪长玢岩和二长斑岩形成构造环境判别图解

Fig.8　Tectonic discrimination diagram of diorite porphyry and monzonite porphyry in Liujiushan Cu deposit

5 结论

本文通过大兴安岭东坡中北段六九山铜矿床成矿系统浅成岩地质、锆石U-Pb同位素定年和元素地球化学特征研究,讨论了成岩时代、成因类型与地球动力学背景,取得的主要认识如下:

1)将浅成岩地质与锆石U-Pb同位素定年相结合,确定闪长玢岩和二长斑岩岩浆就位发生在132 Ma,结合辉钼矿Re-Os同位素年龄((134.1±0.8)Ma),限定成矿发生在早白垩世。

2)元素地球化学特征揭示,闪长玢岩为典型岛弧钙碱性岩,二长斑岩为典型埃达克质岩,二者与成矿作用密切相关;岩浆起源于与大洋板块俯冲有关的以流体交代为主的富集地幔部分熔融。

3)从区域地球动力学角度出发,成岩成矿作用适值中生代早白垩世库拉板块向欧亚板块俯冲的大陆边缘岩浆弧背景。

参考文献(References):

[1] 翟明国,胡波. 矿产资源国家安全、国际争夺与国家战略之思考[J]. 地球科学与环境学报,2021,43(1):1-11.
Zhai Mingguo, Hu Bo. Thinking to State Security, International Competition and National Strategy of Mineral Resources[J]. Journal of Earth Sciencesand Environment, 2021, 43 (1): 1-11.

[2] 李德胜.黑龙江省龙江县后六九铜钼矿床地质特征及成因初探[J]. 矿产与地质,2003,17(增刊):354-357.
Li Desheng. Geological Character and Primary Study of Genesis About Houliujiu Copper-Molybdenum Deposit in Longjiang County of Heilongjiang Province[J]. Mineral Resources and Geology, 2003, 17 (Sup.): 354-357.

[3] 宫永吉,孙景贵,刘阳. 再论大兴安岭中东部六九山铜矿床成矿地质特征、成因与成矿地质背景[J].吉林地质,2020,39(4):1-10.
Gong Yongji, Sun Jinggui, Liu Yang. A Re-Evaluation on the Deposit Geological Features, Genesis and Metallogenic Geological Setting of Liujiushan Cu Deposit in the Central-Eastern Segment of the Greater Xing'an Range[J]. Jilin Geology, 2020,39 (4): 1-10.

[4] 孙景贵,刘阳,徐智恺,等.试论中国东北部陆缘晚中生代浅成热液大规模成矿与深部地质过程对成矿制约[J].吉林大学学报(地球科学版),2023,53(3):651-692.
Sun Jinggui, Liu Yang, Xu Zhikai, et al. Large-Scale Epithermal Mineralization of Late Mesozoic and the Constraints of Deep Geological Processes on Mineralization in the Continental Margin of NE China [J]. Journal of Jilin University (Earth Science Edition), 2023, 53 (3): 651-692.

[5] Williams I S. U-Th-Pb Geochronology by Ion-Microprobe, Applications of Microanalytical Techniques to Understanding Mineralizing Processes [J]. Economic Geology, 1998, 7: 1-35.

[6] Li X H. Geochemistry of the Longsheng Ophiolite from the Southern Margin of Yangtze Craton, SE China[J]. Geological Journal, 1997, 31: 323-338.

[7] 杨元江,吕长禄,李科,等. 黑龙江六九铜矿区岩浆岩年代学及成矿指示意义[J].矿物岩石,2021,41(3):118-127.
Yang Yuanjiang, Lü Changlu, Li Ke, et al. Magmatic Geochronology and Metallogenic Geological Significance in Liujiu Cu Deposit of Heilongjiang Province[J]. Mineralogy and Petrology, 2021, 41 (3): 118-127.

[8] Corfu F, Hanchar J M, Hoskin P W O, et al. Atlas of Zircon Textures[J]. Reviews in Mineralogy and Geochemistry, 2003, 53: 469-500.

[9] Middlemost E A K. Naming Materials in the Magma/Igneous Rock System[J]. Earth Science Reviews, 1994, 37: 215-224.

[10] Peccerillo A, Taylor A R. Geochemistry of Eocene Calc-Alkaline Volcanic Rocks from the Kastamonu Area, Northern Turkey[J]. Contributions to Mineralogy and Petrology, 1976, 58: 63-81.

[11] Sun S S, Mcdonough W F. Chemical and Isotopic Systematics of Oceanic Basalts: Implications for Mantle Composition and Processes[J]. Geological Society London Special Publications, 1989, 42(1): 313-345.

[12] Boynton W V. Geochemistry of the Rare Earth Elements: Meteorite Studies[M]// Henderson P E. Rare Earth Element Geochemistry. Amsterdam: Elsevier,1984: 63-114.

[13] Pearce J A, Kempton P D, Nowell G M, et al. Hf-Nd Element and Isotope Perspective on the Nature and Provenance of Mantle and Subduction Components in Western Pacific Arc-Basin Systems [J]. Journal of Petrology, 1999, 40: 1579-1611.

[14] 赵振华,王强,熊小林.俯冲带复杂的壳幔相互作用

[J].矿物岩石地球化学通报,2004,23(4):277－284.
Zhao Zhenhua, Wang Qiang, Xiong Xiaolin. Complex Mantle-Crust Interaction in Subduction Zone[J]. Bulletin of Mineralogy, Petrology and Geochemistry, 2004, 23(4): 277－284.

[15] Foley S. Petrological Characterization of the Source Components of Potassic Magmas: Geochemical and Experimental Constraints [J]. Lithos, 1992, 28: 187－204.

[16] 赵振华,熊小林,王强,等. 铌与钽的某些地球化学问题[J].地球化学,2008,37(4):304－320.
Zhao Zhenhua, Xiong Xiaolin, Wang Qiang, et al. Some Aspects on Geochemistry of Nb and Ta[J]. Geochimica, 2008,37(4): 304－320.

[17] 邓昌州. 大兴安岭北部中生代斑岩铜矿：成岩与成矿[D]. 长春:吉林大学,2019:1－194.
Deng Changzhou. Petrology and Metallogenesis of the Porphyry Cu Deposits in the Northern Great Xing'an Range[D]. Changchun: Jilin University, 2019: 1－194.

[18] 古阿雷.大兴安岭中东部地区浅成热液-斑岩铜多金属成矿系统成矿地质过程及成矿模式研究[D]. 长春:吉林大学,2016:1－128.
Gu Alei. Study on the Mineralization Processes and Metallogenic Model of Epithermal-Porphyry Copper-Polymetallic Mineralization System in the Central and Eastern of Great Xing'an Range, China[D]. Changchun: Jilin University, 2016: 1－128.

[19] Chiaradia M, Schaltegger U, Spikings R, et al. How Accurately Can We Date the Duration of Magmatic－Hydrothermal Events in Porphyry Systems?: An Invited Paper[J]. Economic Geology, 2013, 108: 565－584.

[20] Chiaradia M, Schaltegger U, Spikings R. Time Scales of Mineral Systems: Advances in Understanding over the Past Decade[J]. Society of Economic Geologists, Special Publication, 2014, 18: 37－58.

[21] Ouyang H G, Wu X L, Mao J W, et al. The Nature and Timing of Ore Formation in the Budunhua Copper Deposit, Southern Great Xing'an Range: Evidence from Geology, Fluid Inclusions, and U－Pb and Re－Os Geochronology[J]. Ore Geology Reviews, 2014, 63: 238－251.

[22] Shi K T, Wang K Y, Ma X L, et al. Fluid Inclusions, C－H－O－S－Pb Isotope Systematics, Geochronology and Geochemistry of the Budunhua Cu Deposit, Northeast China: Implications for Ore Genesis[J]. Geoscience Frontiers, 2020, 11: 1145－1161.

[23] Deng C Z, Sun D Y, Han J S, et al. Ages and Petrogenesis of the Late Mesozoic Igneous Rocks Associated with the Xiaokele Porphyry Cu－Mo Deposit, NE China and Their Geodynamic Implications[J]. Ore Geology Reviews, 2019, 107: 417－433.

[24] Sun Y G, Li B L, Ding Q F, et al. Timing and Ore Formation of the Xiaokele Porphyry Cu (－Mo) Deposit in the Northern Great Xing'an Range, NE China: Constraints from Geochronology, Fluid Inclusions, and H－O－S－Pb Isotopes[J]. Ore Geology Reviews, 2022, 143: 104806.

[25] Sun Y G, Li B L, Zhao Z H, et al. Age and Petrogenesis of Late Mesozoic Intrusions in the Huoluotai Porphyry Cu－(Mo) Deposit, Northeast China: Implications for Regional Tectonic Evolution [J]. Geoscience Frontiers, 2022, 13: 101344.

[26] Deng C Z, Sun D Y, Han J S, et al. Late-Stage Southwards Subduction of the Mongol-Okhotsk Oceanic Slab and Implications for Porphyry Cu－Mo Mineralization: Constraints from Igneous Rocks Associated with the Fukeshan Deposit, NE China[J]. Lithos, 2019, 326/327: 341－357.

[27] Sun Y G, Li B L, Ding Q F, et al. Mineralization Age and Hydrothermal Evolution of the Fukeshan Cu (Mo) Deposit in the Northern Great Xing'an Range, Northeast China: Evidence from Fluid Inclusions, H－O－S－Pb Isotopes, and Re－Os Geochronology [J]. Minerals, 2020, 10: 591.

[28] Zhao Q Q, Zhai D G, Mathur R, et al. The Giant Chalukou Porphyry Mo Deposit, Northeast China: The Product ofa Short-Lived, High Flux Mineralizing Event[J]. Economic Geology, 2021, 116: 1209－1225.

[29] 季根源,江思宏,李高峰,等. 大兴安岭南段毛登 Sn－Cu 矿床岩浆作用对成矿制约:年代学、地球化学及 Sr－Nd－Pb 同位素证据[J]. 大地构造与成矿学, 2021,45(4):681－704.
Ji Genyuan, Jiang Sihong, Li Gaofeng, et al. Metallogenetic Control of Magmatism on the Maodeng Sn－Cu Deposit in the Southern Great Xing'an Range: Evidence from Geochronology, Geochemistry, and Sr－Nd－Pb Isotopes[J]. Geotectonica et Metallogenia, 2021, 45(4): 681－

704.

[30] 潘小菲,郭利军,王硕,等. 内蒙古维拉斯托铜锌矿床的白云母 Ar/Ar 年龄探讨[J]. 岩石矿物学杂志,2009,28(5):473-479.
Pan Xiaofei, Guo Lijun, Wang Shuo, et al. Laser Microprobe Ar-Ar Dating of Biotite from the Weilasituo Cu-Zn Polymetallic Deposit in Inner Mongolia[J]. Acta Mineralogica et Petrologica, 2009, 28(5): 473-479.

[31] Liu Y F, Jiang S H, Bagas L. The Genesis of Metal Zonation in the Weilasituo and Bairendaba Ag-Zn-Pb-Cu-(Sn-W) Deposits in the Shallow Part of a Porphyry Sn-W-Rb System, Inner Mongolia, China[J]. Ore Geology Reviews, 2016, 78: 150-173.

[32] Wang F X, Bagas L, Jiang S H, et al. Geological, Geochemical, and Geochronological Characteristics of Weilasituo Sn-Polymetal Deposit, Inner Mongolia, China[J]. Ore Geology Reviews, 2017, 80: 1206-1229.

[33] Gu A L, Sun J G, Bai L A, et al. Petrogenesis and Metallogenesis of the Early Cretaceous Naoniushan Cu-Dominated Polymetallic Deposit in the Central Great Xing'an Range, NE China[J]. Journal of Asian Earth Sciences, 2018, 165: 114-131.

[34] Wang X D, Xu D M, Lü X B, et al. Origin of the Haobugao Skarn Fe-Zn Polymetallic Deposit, Southern Great Xing'an Range, NE China: Geochronological, Geochemical, and Sr-Nd-Pb Isotopic Constraints[J]. Ore Geology Reviews, 2018, 94: 58-72.

[35] Sun Q F, Wang K Y, Wang Y C, et al. Fluid Evolution and Ore Genesis of the Chaobuleng Skarn Fe-Zn Polymetallic Deposit, Northeast China: Evidence from Fluid Inclusions, C-O-S-Pb Isotopes, and Geochronology[J]. Journal of Geochemical Exploration, 2021, 227: 106796.

[36] Wu C, Wang B R, Zhou Z G, et al. The Relationship Between Magma and Mineralization in Chaobuleng Iron Polymetallic Deposit, Inner Mongolia[J]. Gondwana Research, 2017, 45: 228-253.

[37] 江思宏,聂凤军,刘翼飞,等. 内蒙古孟恩陶勒盖银多金属矿床及其附近侵入岩的年代学[J]. 吉林大学学报(地球科学版),2011,41(6):1755-1769.
Jiang Sihong, Nie Fengjun, Liu Yifei, et al. Geochronology of Intrusive Rocks Occurring in and Around the Mengentaolegai Silver-Polymetallic Deposit, Inner Mongolia[J]. Journal of Jilin University (Earth Science Edition), 2011, 41(6): 1755-1769.

[38] 李铁刚,武广,刘军,等. 大兴安岭北部甲乌拉铅锌银矿床 Rb-Sr 同位素测年及其地质意义[J]. 岩石学报,2014,30(1):257-270.
Li Tiegang, Wu Guang, Liu Jun, et al. Rb-Sr Isochron Age of the Jiawula Ag-Pb-Zn Deposit in the Manzhouli Area and Its Geological Significance[J]. Acta Petrologica Sinica, 2014, 30(1): 257-270.

[39] Niu S D, Li S R, Huizenga J M, et al. Zircon U-Pb Geochronology and Geochemistry of the Intrusions Associated with the Jiawula Ag-Pb-Zn Deposit in the Great Xing'an Range, NE China and Their Implications for Mineralization[J]. Ore Geology Reviews, 2017, 86: 35-54.

[40] 明珠,孙景贵,闫佳,等. 内蒙古东部得耳布尔铅锌矿床安山岩的形成环境和岩浆热液演化史:锆石 U-Pb 定年[J]. 世界地质,2015,34(3):590-598.
Ming Zhu, Sun Jinggui, Yan Jia, et al. Forming Environment and Magmatic-Hydrothermal Evolution History of Andesite in Derbur Lead-Zinc Deposit of Eastern Inner Mongolia: Zircon U-Pb Dating[J]. Global Geology, 2015, 34(3): 590-598.

[41] 赵岩,吕骏超,张德宝,等. 内蒙古东北部得耳布尔铅锌银矿床闪锌矿 Rb-Sr 年龄及地质意义[J]. 矿床地质,2017,36(4):893-904.
Zhao Yan, Lü Junchao, Zhang Debao, et al. Rb-Sr Isochron Age of Derbur Pb-Zn-Ag Deposit in Erguna Massif of Northeast Inner Mongolia and Its Geological Significance[J]. Mineral Deposits, 2017, 36(4): 893-904.

[42] Xu Z T, Sun J G, Liang X L, et al. Genesis of Ore-Bearing Volcanic Rocks in the Derbur Lead-Zinc Mining Area of the Erguna Massif, Western Slope of the Great Xing'an Range, NE China: Geochemistry, Sr-Nd-Pb Isotopes, and Zircon U-Pb Geochronology[J]. Geological Journal, 2019, 54: 3891-3908.

[43] Li T G, Wu G, Liu J, et al. Geochronology, Fluid Inclusions and Isotopic Characteristics of the Chaganbulagen Pb-Zn-Ag Deposit, Inner Mongolia, China[J]. Lithos, 2016, 261: 340-355.

[44] Jiang S H, Chen C L, Bagas L, et al. Two Mineralization Events in the Baiyinnuoer Zn-Pb Deposit in Inner Mongolia, China: Evidence from

Field Observations, S-Pb Isotopic Compositions and U-Pb Zircon Ages[J]. Journal of Asian Earth Sciences, 2017, 144: 339-367.

[45] Xu Z K, Sun J G, Xu Z T, et al. Fluid Inclusion and Isotopic Constraints on the Origin of the Ag-Pb-Zn Polymetallic Mineralization at Biliya, Great Xing'an Range, NE China[J]. Ore Geology Reviews, 2022, 143: 104793.

[46] Xu Z T, Liu Y, Sun J G, et al. Nature and Ore Formation of the Erdaohezi Pb-Zn Deposit in the Great Xing'an Range NE China[J]. Ore Geology Reviews, 2020, 119: 103385.

[47] Xu Z T, Sun J G, Liang X L, et al. Geochronology, Geochemistry, and Pb-Hf Isotopic Composition of Mineralization-Related Magmatic Rocks in the Erdaohezi Pb-Zn Polymetallic Deposit, Great Xing'an Range, Northeast China[J]. Minerals, 2020, 10: 274.

[48] Zeng Q D, Liu J M, Chu S X, et al. Re-Os and U-Pb Geochronology of the Duobaoshan Porphyry Cu-Mo-(Au) Deposit, Northeast China, and Its Geological Significance[J]. Journal of Asian Earth Sciences, 2014, 79: 895-909.

[49] 康永建,王亚军,黄光杰,等. 内蒙古八大关斑岩型铜钼矿床成岩成矿年代学研究[J]. 矿床地质,2014,33(4):795-806.
Kang Yongjian, Wang Yajun, Huang Guangjie, et al. Study of Rock-Forming and Ore-Forming Ages of Badaguan Porphyry Cu-Mo Deposit in Inner Mongolia[J]. Mineral Deposits, 2014, 33(4): 795-806.

[50] Pearce J A, Harris B W, Tindle A G. Trace Element Discrimination Diagrams for the Tectonic Interpretations of Granitic Rocks[J]. Journal of Petrology, 1984, 25: 956-983.

[51] King P L, White A J R, Chappell B W, et al. Characterization and Origin of Aluminous A-Type Granites from the Lachlan Fold Belt, Southeastern Australia[J]. Journal of Petrology, 1997, 38: 371-391.

[52] Chappell B W. Aluminium Saturation in I- and S-Type Granites and the Characterization of Fractionated Haplogranites[J]. Lithos, 1999, 46(3): 53-551.

[53] Chappell B W, White A J R. Two Contrasting Granite Types: 25 Years Later[J]. Australian Journal of Earth Sciences, 2001, 48(4): 489-499.

[54] Wu F Y, Sun D Y, Li H, et al. A-Type Granites in Northeastern China: Age and Geochemical Constraints on Their Petrogenesis[J]. Chemical Geology, 2002, 187(1): 143-173.

[55] Sengör A M C, Natal'in B A, Burtman V S. Evolution of the Altaid Tectonic Collage and Paleozoic Crustal Growth in Eurasia[J]. Nature, 1993, 364: 299-307.

[56] Jahn B M. The Central Asian Orogenic Belt and Growth of the Continental Crust in the Phanerozoic[J]. Geological Society, London: Special Publications, 2004, 226: 73-100.

[57] 董清水,何春生,楼仁兴,等. 大兴安岭南段阿鲁科尔沁旗地区林西组沉积环境特征及其时限的地质意义[J]. 吉林大学学报(地球科学版),2020,50(2):425-441.
Dong Qingshui, He Chunsheng, Lou Renxing, et al. Geological Significance of Sedimentary Environment Characteristics and Time Limit of Linxi Formation in Arhorchin Banner, Southern Great Xing'an Range[J]. Journal of Jilin University (Earth Science Edition), 2020, 50(2): 425-441.

[58] Windley B F, Alexeiev D, Xiao W J, et al. Tectonic Models for Accretion of the Central Asian Orogenic Belt[J]. Journal of the Geological Society, 2007, 164: 31-47.

[59] Wu F Y, Sun D Y, Ge W C, et al. Geochronology of the Phanerozoic Granitoids in Northeastern China[J]. Journal of Asian Earth Sciences, 2011, 41(1): 1-30.

[60] 孙德有,吴福元,高山,等. 吉林中部晚三叠世和早侏罗世两期铝质A型花岗岩的厘定及对吉黑东部构造格局的制约[J]. 地学前缘,2005,12(2): 263-275.
Sun Deyou, Wu Fuyuan, Gao Shan, et al. Confirmation of Two Episodes of A-Type Granite Emplacement During Late Triassic and Early Jurassic in the Central Jilin Province, and Their Constraints on the Structural Pattern of Eastern Jilin-Heilongjiang Area, China[J]. Earth Science Frontiers, 2005, 12(2): 263-275.

[61] 尹志刚,庞学昌,王春生,等. 小兴安岭南部早侏罗世二长花岗岩形成时代、地球化学特征及地质意义[J]. 地质通报,2020,39(1):27-39.
Yin Zhigang, Pang Xuechang, Wang Chunsheng, et al. Formation Age, Geochemical Characteristics and Geological Significance of the Early Jurassic Monzonitic Granites in Southern Xiao Hinggan

Mountains[J]. Geological Bulletin of China, 2020, 39(1): 27-39.

[62] 郑全波,汪岩,张广宇,等. 黑龙江东部晚三叠世A型花岗岩的厘定及其构造环境的地球化学制约[J].世界地质,2019,31(3):471-478.
Zheng Quanbo, Wang Yan, Zhang Guangyu, et al. Confirmation of Late Triassic A-Type Granite and Their Geochemical Constraints on Structural Setting in Eastern Heilongjiang[J]. Global Geology, 2019, 31(3): 471-478.

[63] 徐智涛,李萌萌,孙景贵,等. 大兴安岭得耳布尔地区中侏罗世流纹岩成因及成岩地球动力学背景[J].吉林大学学报(地球科学版),2023,53(3):866-886.
Xu Zhitao, Li Mengmeng, Sun Jinggui, et al. Genesis and Diagenetic Geodynamic Background of Middle Jurassic Rhyolites in Derbur Area, Great Xing'an Range[J]. Journal of Jilin University (Earth Science Edition), 2023, 53(3): 866-886.

[64] Shu Q H, Chang Z S, Lai Y, et al. Regional Metallogeny of Mo-Bearing Deposits in Northeastern China, with New Re-Os Dates of Porphyry Mo Deposits in the Northern Xilamulun District[J]. Economic Geology, 2016, 111: 1783-1798.

[65] Pearce J A, Harris N B W, Tindle A G. Trace Element Discrimination Diagrams for the Tectonic Interpretation of Granitic Rocks[J]. Journal of Petrology, 1984, 25: 956-983.